# Chapter 17
# A Regenerative Approach to Energy Efficient Hydraulic Vibration Control

**Jonathan L. du Bois**

**Abstract** Active vibration control technologies are reaching maturity in many applications, in both periodic and transient operating regimes. Historically these systems have been designed without regard for the power they consume, which is not only inefficient and costly, but limits their adoption in applications where it is impractical to provide large power supplies. Strategies for reducing power consumption include semi-active and regenerative methods. The former limits the device action to dissipative forces, through adjustable spring and/or damping rates. The latter uses the dissipative portion of the cycle to store energy in a reservoir, which can then be used in the remainder of the cycle. This paper looks at the benefits of using hydraulic devices in this context instead of the prevalent electromechanical devices. A case study of regenerative hydraulic vibration control is presented using digital hydraulics concepts, analogous to the switching power supplies and amplifiers that have revolutionised the efficiency of modern electronic equipment. The limitations and trade-offs are examined and projections are made as to the performance that could be achieved as the limitations of contemporary hydraulic components are improved upon.

**Keywords** Active vibration control • Regenerative damper • Digital hydraulics • Seismic • Earthquake

## 17.1 Introduction

Active vibration control is a well established field, and books and papers on the topic abound [1, 2]. Where energy supply is scarce, typically semiactive control is employed [3]. More recently, regenerative concepts have started to appear, where instead of dissipating vibration energy, a vibration mitigation device absorbs the energy from the structure and stores it for use in fully-active portions of the control strategy. Typically such devices are advocated for automotive use and store the energy in electrical form, using electro-mechanical means to convert stored energy to and from motion [4–6].

Hydraulic devices have advantages over other technologies: principally in the range of their power density. Large forces can be generated with high velocity, making them suitable for heavy duty applications, for example the focus of this study which is the motion control of large buildings. The drawback of hydraulic devices in this context is their efficiency. The more-or-less ubiquitous approach to pressure modulation in hydraulic systems is to use a proportional valve, throttling the flow and dissipating large amounts of energy in turbulence and ultimately viscous heat losses. If energy is to be conserved in the device, flow throttling is clearly an untenable approach. The prospect of using regenerative hydraulic systems helps to address one of the major concerns in implementing active vibration control for the mitigation of seismic response in buildings: that of continued operation in the event of power failure.

Digital hydraulic methods employ discrete elements in an effort to mitigate effects such as these. In particular, fast valve switching can be employed to create a device which modulates the output pressure in proportion to the duty cycle of the valve: in essence a pulse-width modulated (PWM) control [7]. The approach is used in a crude form in the hydraulic ram pump [8]. An analogy can be drawn between the emerging digital hydraulic methods and the evolution of efficient Class D amplifiers and switched-mode power supplies in the electrical world. In the case of the latter, fast switching transistors

J.L. du Bois (✉)
Department of Mechanical Engineering, University of Bath, Claverton Down, Bath, BA2 7AY, UK
e-mail: j.l.du.bois@bath.ac.uk

G. Foss and C. Niezrecki (eds.), *Special Topics in Structural Dynamics, Volume 6: Proceedings of the 32nd IMAC, A Conference and Exposition on Structural Dynamics, 2014*, Conference Proceedings of the Society for Experimental Mechanics Series,
DOI 10.1007/978-3-319-04729-4_17, 

offered a revolution which made the technology possible, whereas for hydraulic systems continued efforts to improve on valve switching speeds are pushing the envelope to the point where the technology presented in this paper is feasible.

The work in this paper sets out the case for the use of digital hydraulic control in regenerative active vibration control. The principle is to improve the efficiency of energy harvesting in hydraulic devices through the use of fast-switching valves and analogue filtering elements to approach active vibration control performance without the need for an external hydraulic power supply.

## 17.2 Active Control

The work of Lazar et al. [9] shows that while semi-active vibration control approaches can come close to the performance of fully-active systems, the performance is significantly enhanced if the passivity constraint is relaxed. A semi-active device cannot input power to the system so the passivity constraint is

$$p(t) = u_{MR} v_{MR} \leq 0 \tag{17.1}$$

where $u_{MR}$ is the control force applied by the device and $v_{MR}$ is the relative velocity between the attachment points. Lazar et al. demonstrate that significant improvements can be achieved by imbuing the device with limited fully-active capabilities:

$$p(t) = u_{MR} v_{MR} \leq \gamma p_A \tag{17.2}$$

where $p_A$ is the maximum power dissipation of the device and $\gamma$ is a value between 0 and 1 governed by the efficiency of the energy harvesting, or regeneration processes. (NB the definition here is subtly different from that of Lazar et al. but follows on naturally from their demonstration.) Their findings indicate that a value of $\gamma = 0.75$ produces results that would be indistinguishable from a fully active system for practical purposes. Hence, the objective in this work is to demonstrate in principle a methodology for regenerative vibration control that can achieve this level of performance in a hydraulic device.

Following the methods of reference [9], a two degree-of-freedom (DOF) model of a small two-storey building is simulated. The same model parameters are used here, so that the mass of each floor slab is 500 kg and the frame beams create a stiffness of 3,500 kN/m between each storey. Damping is included to produce a modal damping ratio of 5%. Linear quadratic regulator theory [10] is applied to determine gains for a full-state-feedback controller, to give

$$u(t) = -\begin{bmatrix} 21.4065 & -18.0327 & 0.3436 & 0.1322 \end{bmatrix} \begin{Bmatrix} x_1 \\ x_2 \\ \dot{x}_1 \\ \dot{x}_2 \end{Bmatrix} \tag{17.3}$$

Figure 17.1 shows the response of the uncontrolled system and the actively controlled system to a chirp signal ranging from 1 to 20 Hz. The frequency increases linearly with time over the 100 s so the peak at ~40 s corresponds to the natural frequency at 8.23 Hz. Figure 17.2 shows the power input to the structure from the active control system. While the overall effect of the active control is to dissipate power, there is a non-negligible amount of power input to the system for segments of its operation. This supports the idea of storing energy during the dissipative part of the cycle and returning some of that energy to the structure at the appropriate points in the cycle. The fact that the active control device dissipates energy on aggregate means that there is scope for efficiency losses in the energy conversion and storage processes, making the proposition herein a realistic one.

## 17.3 Hydraulic Buck Converter

Figure 17.3 shows a schematic for the hydraulic equivalent of what would be called a Buck Converter in an electrical context. It steps down from a high pressure reservoir to low pressure with minimal loss of total pressure, thus conserving energy. The system is closed-circuit, so the energy storage takes the form of a symmetric, dual-chamber piston with a spring on the piston rod acting as the energy storage element. A servovalve is used to provide a pulse width modulated pressure according to the

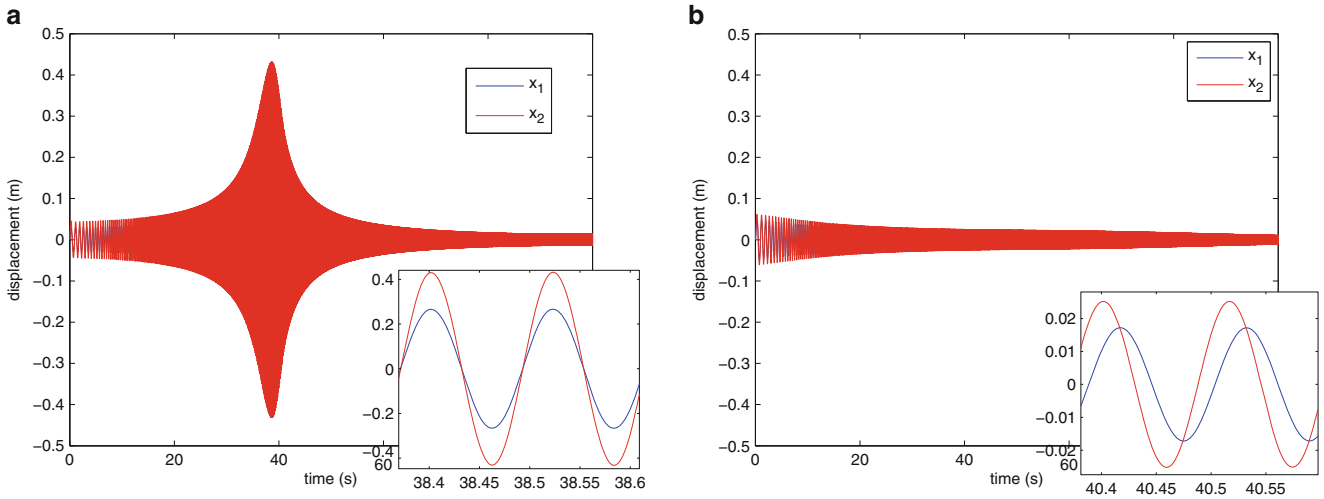


**Fig. 17.1** Response of structure to chirp acceleration input from 1 to 20 Hz, with the passive structure alone compared to the active control scheme. (**a**) Uncontrolled; (**b**) active control

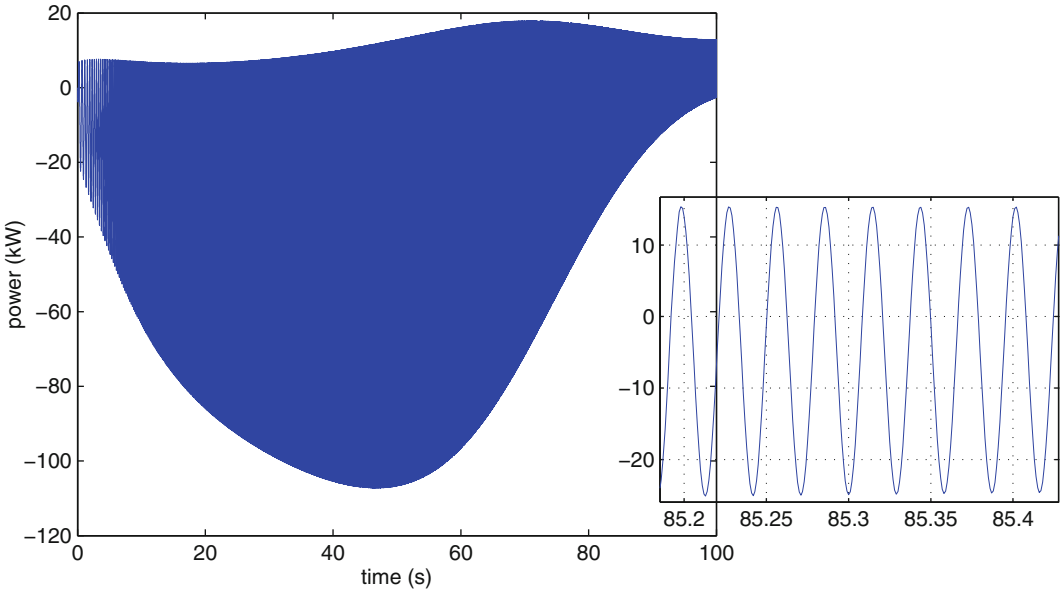


**Fig. 17.2** Power input to system from active control

required output pressure, and this pressure is filtered by means of an inertance tube and a pair of accumulators to give a smoothed pressure output. This then drives a piston for the purpose of the vibration control, represented in the diagram as a dissipative load.

The biggest limiting factor in the performance fast-switching hydraulic circuits is the valve response. Recent advancements have seen high flow rates combined with switching times of ∼1 ms [11, 12]. Correspondingly, in this study the valve dynamics are modelled with a second order transfer function, with undamped natural frequency of $\omega_0 = 500$ Hz and a damping ratio of $\zeta = 0.75$. The output of the transfer function is set to saturate at 0 and 1 for the lower and upper limits, respectively. The resulting step response can be seen in Fig. 17.4.

Pressure losses across the valve orifice are modelled by means of a turbulent orifice flow, with the relationship

$$\Delta p \propto Q|Q| \tag{17.4}$$

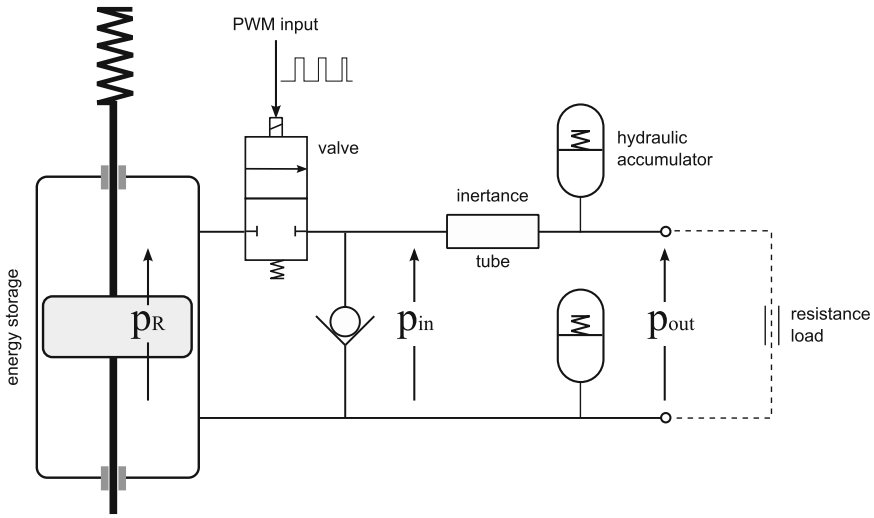


**Fig. 17.3** Schematic for a hydraulic buck converter

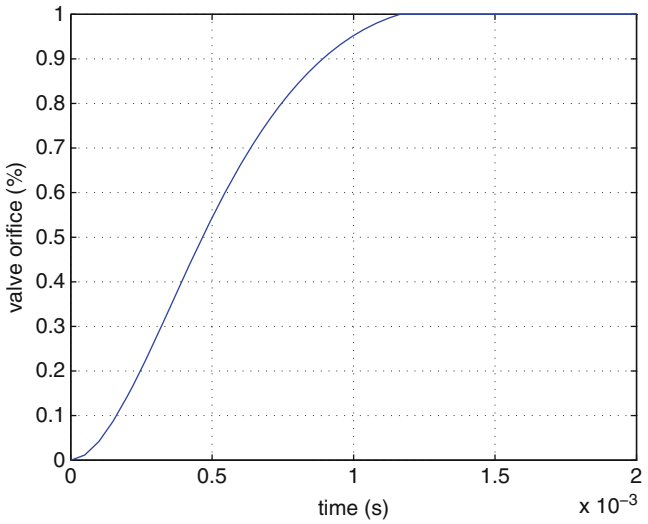


**Fig. 17.4** Step response for the hydraulic valve

where $\Delta p$ is the pressure loss and $Q$ is the volumetric flow rate through the valve (incompressible assumptions are made for the hydraulic fluid throughout this analysis). When fully open, from [12], a loss coefficient of $20 \times 10^8$ can be achieved, and from [13] the loss coefficient is found to be inversely proportional to the square of the orifice area.

The inertance tube's dynamics are described as a single state system by

$$A\Delta p = m\ddot{x} \tag{17.5}$$

where $A$ is the tube area, $\Delta p$ is the pressure difference across the tube, $m$ is the mass of fluid in the tube, and $\ddot{x}$ is the acceleration of the fluid in the tube. From this,

$$Q_I = \frac{A}{\rho L}\int \Delta p \mathrm{dt} \tag{17.6}$$

where $Q_I$ is the flow through the tube, $\rho$ is the density of the fluid, and $L$ is the length of the tube.

The accumulators act as one in this model due to the incompressibility assumption and the closed-circuit configuration (with no other compressible elements included in the circuit). They can be described in terms of their combined pressure-charge characteristic,

$$p_A = k_A \int Q \mathrm{dt} \tag{17.7}$$

where $k_A$ is a linear coefficient for the accumulators and $\int Q\mathrm{d}t$ is the volumetric charge of the accumulators. The pressure $p_A$ is the pressure differential between the two accumulators and the charge represents the volume displaced from the lower to the upper accumulator.

These two components comprise the filter for smoothing out the PWM pressures from the valve. The relationship between the input pressure $p_{in}$ and the output pressure $p_{out}$ is described by

$$p_{out} = p_A = k_A \int (Q_I - Q_L)\mathrm{d}t \tag{17.8}$$

or

$$p_{out} = k_A \int \left( \frac{A}{\rho L} \int \Delta p \mathrm{d}t - Q_L \right) \mathrm{d}t \tag{17.9}$$

where $Q_L$ is the flow through the load attached to the output of the buck converter. The pressure across the inertance tube, $\Delta p$ is given by

$$\Delta p = p_{in} - p_{out} \tag{17.10}$$

and the output load is assumed to have a linear pressure-flow relationship so that

$$p_{out} = k_A \int \left( \frac{A}{\rho L} \int (p_{in} - p_{out})\mathrm{d}t - \frac{p_{out}}{c_L} \right) \mathrm{d}t \tag{17.11}$$

where $c_L$ is the laminar loss coefficient associated with the dissipative load. This can be rearranged to

$$\frac{\rho L}{A k_A} \ddot{p}_{out} + \frac{\rho L}{A c_L} \dot{p}_{out} + p_{out} = p_{in} \tag{17.12}$$

Or in the frequency domain,

$$P_{out}(s) = \frac{1}{\frac{\rho L}{A k_A} s^2 + \frac{\rho L}{A c_L} s + 1} P_{in}(s) \tag{17.13}$$

This is a second order system where

$$\omega_0{}^2 = \frac{A k_A}{\rho L} \qquad \text{and} \qquad \frac{2\zeta}{\omega_0} = \frac{\rho L}{A c_L} \tag{17.14}$$

To prevent undesirable oscillation, a critical damping ratio is used so $\zeta = 1$ and

$$\omega_0 = \frac{2 A c_L}{\rho L} = \sqrt{\frac{A k_A}{\rho L}} \tag{17.15}$$

Now stipulating a cutoff frequency for the filter, $\omega_0 = 2\pi f_c$,

$$k_A = 4 \frac{A}{\rho L} c_L{}^2 \qquad \text{and} \qquad \pi f_c = \frac{A c_L}{\rho L} \tag{17.16}$$

and finally, combining these gives

$$k_A = 4\pi f_c c_L \qquad \text{and} \qquad \frac{A}{\rho L} = \frac{\pi f_c}{c_L} \tag{17.17}$$

This determines the constants for the accumulators and for the inertance tube dependent upon the filter cutoff frequency (i.e. the maximum operating frequency of the vibration control device) and the expected load characteristics of the structure whose vibrations are being controlled. In practice this will vary dramatically throughout operation, but this analysis gives a starting point for assigning some values. The peak load characteristic should be used as increasing the load for a given set of component parameters will cause the system to be underdamped (from Eq. (17.14)).

The drawback of assuming too high a value for the cutoff frequency is that the unwanted harmonics of the PWM carrier frequency, known as pressure ripple, will become more pronounced in the output pressure (and resultant piston force), while the drawback of a low cutoff frequency is that it will impinge on the bandwidth of the device in operation. The obvious solution is to increase the PWM carrier frequency, but this is limited by the response time of the hydraulic valve. Setting the carrier frequency too high for the valve results in a controller that fails to track the reference signal and suffers from reduced efficiency on account of the greater proportion of the cycle spent with the valve between states.

## 17.4 Hydraulic Component Sizing

From Fig. 17.2 the peak power input to the structure is just under 18 kW. Using the linear pressure-flow relationship

$$p = c_L Q \tag{17.18}$$

combined with the expression for hydraulic power

$$\Omega = pQ \tag{17.19}$$

where $\Omega$ is the power leaving the device and entering the structure, the equivalent loss coefficient $c_L$ can be found from

$$c_L = \frac{\Omega}{Q^2} = \frac{p^2}{\Omega} \tag{17.20}$$

The equivalent loss coefficient is thus determined by the output piston sizing for the device: it is the piston size that relates the velocity of the structural DOF at peak power to the flow rate in the device. This is seemingly a free choice, but in practice will need careful optimisation. Larger piston areas will result in smaller pressures and larger flow rates, thus giving a small $c_L$ for a given power and velocity. This is beneficial because a small $c_L$ permits shorter inertance tubes and lower stresses on accumulators. Larger flow rates, however, will produce greater losses across valves and other restrictions. Conversely, small piston areas will lead to lower flow rates and higher pressures. The turbulent losses across flow restrictors will be reduced, but the inertance tube will need to be longer and thinner, resulting in greater laminar losses coupled with the spurious elastic and compressible behaviour associated with high pressures. For the purposes of this paper a piston area of

The velocity of the structural DOF coinciding with the peak power is $0.5\,\mathrm{ms}^{-1}$. Moog's current Hydrostatic Bearing Test Actuator range uses a piston area of $86.6\,\mathrm{cm}^2$ for the 160 kN model, which would be needed for the ~125 kN forces seen in this example. A piston area of $86.6 \times 10^{-4}\,\mathrm{m}^2$ at $0.5\,\mathrm{ms}^{-1}$ gives a flow rate of $43.3 \times 10^{-4}\,\mathrm{m}^3\,\mathrm{s}^{-1}$. Using this in Eq. (17.20) with a power of 18 kW gives

$$c_L = \frac{\Omega}{Q^2} = \frac{18 \times 10^3}{(43.3 \times 10^{-4})^2} = 9.6 \times 10^8\ \mathrm{Nsm}^{-5} \tag{17.21}$$

A PWM carrier frequency of 100 Hz is chosen, so that the valve spends ~80% of its time in a fully-open or fully-closed position. A filter cutoff frequency of $f_c = 10$ Hz is used to mitigate the 100 Hz ripple and harmonics thereof. These values are borderline values; ideally greater margins would be desirable but the valve switching speed is the key limitation here. The inertance tube and accumulator sizing is then taken from Eq. (17.17) to give

$$k_A = 1.21 \times 10^{11}\ \mathrm{Nm}^{-5} \qquad \text{and} \qquad \frac{A}{\rho L} = 3.27 \times 10^{-8}\ \mathrm{m}^4\,\mathrm{kg}^{-1} \tag{17.22}$$

This study makes the simplifying assumption of a constant reservoir pressure, justified by the understanding that more energy needs to be dissipated from the structure than returned to it. Two alternative flow paths are included to permit return flow into the reservoir, with the servovalve and check valve in Fig. 17.3 exchanged for the case of flow returning to the energy storage chamber. Finally, when the active force control demand changes direction, a four-port servovalve is used to swap the connectivity of the output pressure and invert the sign of the pressure difference. A reservoir pressure of 150 bar is used to provide a margin over the 125 kN forces required of the $86.6 \times 10^{-4}\,\mathrm{m}^2$ piston.

The PWM control uses a triangular-wave signal compared to the reference pressure signal to determine the on/off state of the pulse. As well as the feedforward pressure demand, there is a proportional feedback controller using the measured pressure output. A gain of 10 is used for the proportional gain.

## 17.5 Results

The force demand from the results of Sect. 17.2 are used, scaled by the output piston area, as the reference signal for the hydraulic transformer. The demand and actual output pressures are shown in Fig. 17.5. Below 3 Hz the device tracks the reference pressure moderately well. There are some artefacts from the abrupt swapping of the output ports at the zero crossing, and the physicality of the behaviour here should be questioned because of the ideal representation of the servovalve used to swap these ports in the model, but overall the tracking is reasonable. Beyond 3 Hz, the performance drops off rapidly. The phase begins to lag, and the switching behaviour at the zero-crossing becomes increasingly problematic. This configuration turns out to be particularly unsuitable as the tracking performance drops off: the momentum in the inertance tube imposes the wrong sign on the time-derivative of the pressure immediately after the zero-crossing of the reference, exacerbating both the spurious transient dynamics and the intrinsic tracking problems. By the time the first resonant frequency is reached at ∼8 Hz, or 40 s, the amplitude has dropped off significantly and the pressure no longer resembles that of the reference signal.

The pressure is low-pass filtered with a cutoff of 500 Hz, then sampled at 1,000 Hz and the resulting spectral decomposition is shown in Fig. 17.6. Some aliasing artefacts remain. But I'm not processing this again now; you get the idea. The reference signal is comprised mainly of a single harmonic frequency, whereas the output pressure is clearly seen to suffer from higher harmonic components with a strong onset at around 3 Hz (15 s) and steady worsening towards the higher frequency bands.

Two observations stand out from these results. The first is that the topology of the device, with a four-port valve used to switch the pressure direction at zero-crossings in the reference, produces unnecessary difficulties in tracking. A potential solution would be to use two such devices in a push–pull arrangement. The second observation is that the switching speeds for the hydraulic valves impose consequential restrictions on the operational bandwidth of the device. With current valve technology the vibration control approach proposed here remains infeasible for frequencies above 1 or 2 Hz.

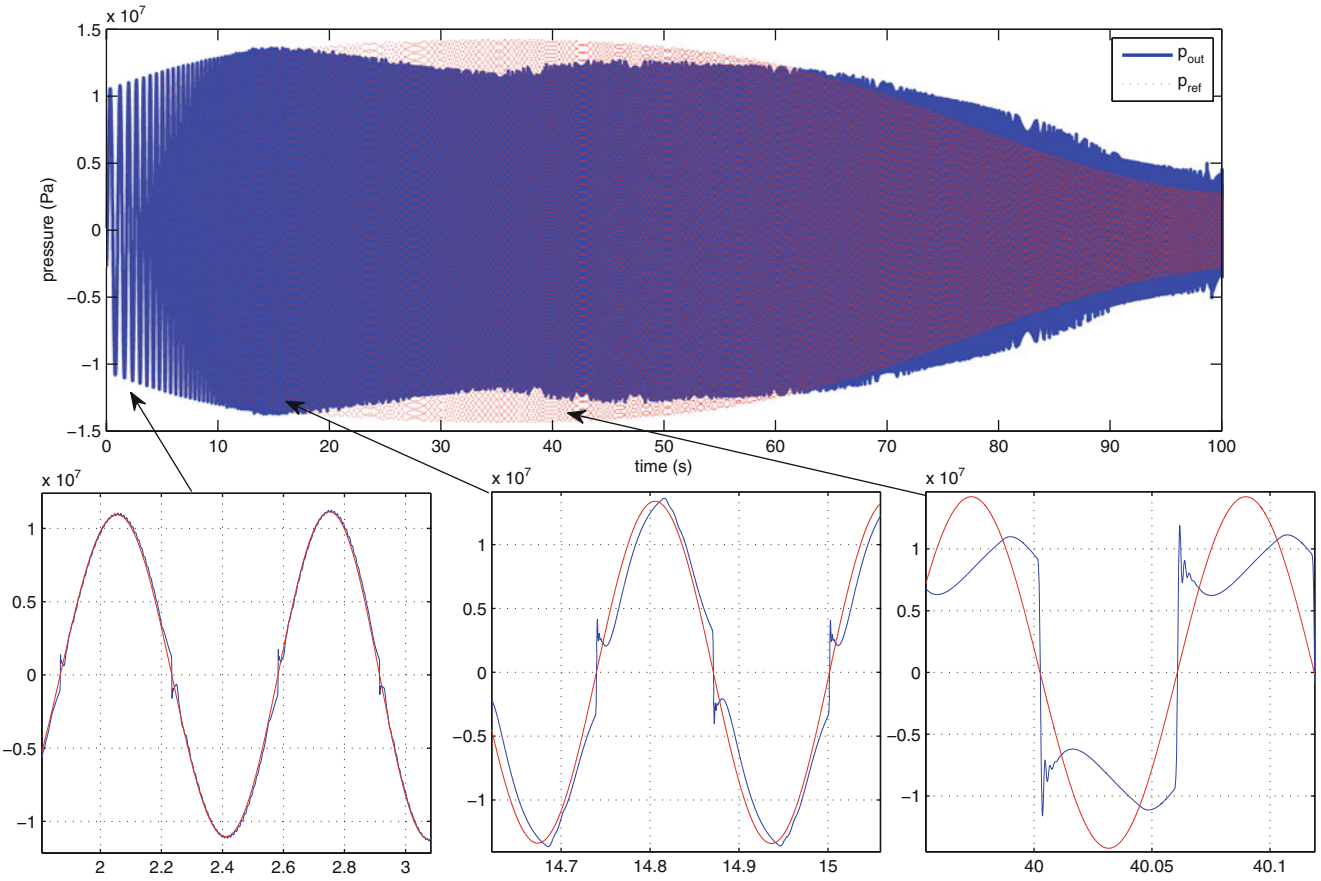


**Fig. 17.5** Reference and output pressure signals

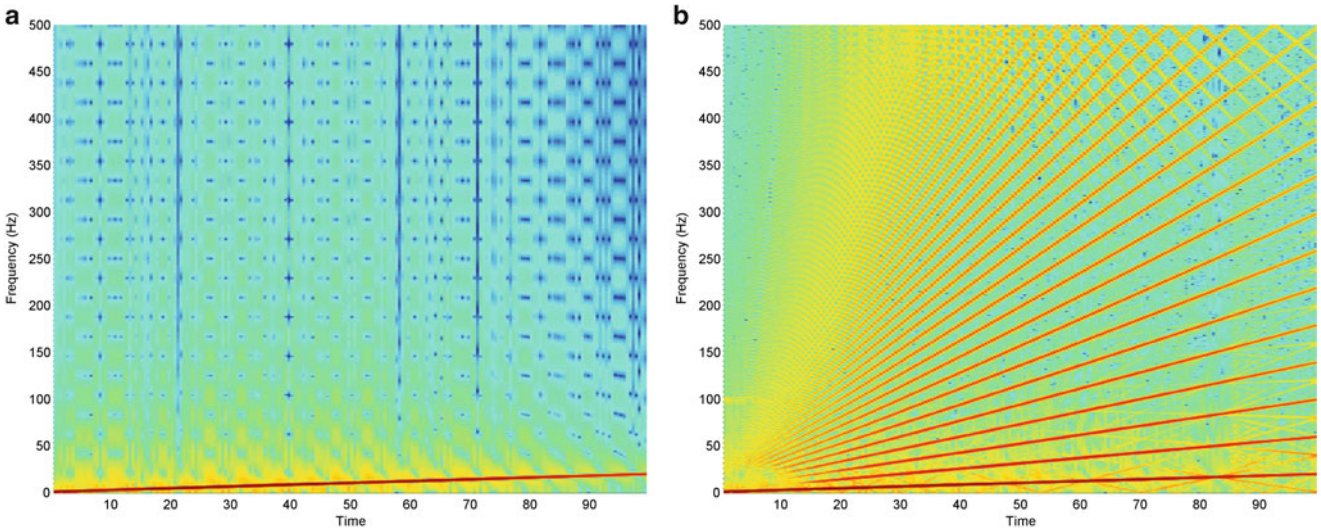


**Fig. 17.6** Spectral decomposition with a STFFT for the reference and output pressures of the hydraulic device. (**a**) Reference pressure; (**b**) output pressure

One final set of results is presented here, exploring the effect of higher valve switching bandwidth. The undamped natural frequency of the valve is changed to 5,000 Hz, exploring the effect of a tenfold increase in the switching speed. The PWM carrier frequency is increased to 1 kHz and the analogue filtering cutoff frequency is raised to 50 Hz. The result, unsurprisingly, is a marked improvement in the pressure tracking. Figure 17.7 shows the time history, while Fig. 17.8 shows the spectral content. It is postulated that this performance would be of a satisfactory level for vibration control in the context of low-frequency seismic response suppression. An immediate target for hydraulic valve performance for this application is thus a switching time of 0.1 ms.

## 17.6 Conclusions

This paper has set out to explore the feasibility of using digital hydraulic concepts to create regenerative vibration control device, capable of harvesting energy to sustain fully-active vibration control without the need for an external hydraulic power supply. Modelling with realistic constraints has been used to evaluate the readiness of the technology in the context of low-frequency (∼0–20 Hz) seismic vibrations in a two-storey building. The following conclusions have been reached.

Firstly, the supporting component technologies are on the verge of maturing to the point where the suggested approach could be implemented. The simulations suggest that for very low frequencies, up to 1 or 2 Hz, the approach *may* already prove feasible. For higher bandwidths, faster valve switching technologies need to evolve to meet the requirements of a system. This study suggests that a tenfold improvement on the existing technology to produce a valve switching time of 0.1 ms would offer the possibility of using these approaches to control vibrations up to 20 Hz or more.

The second conclusion is that the single-switch configuration used here is inadequate for controlling both positive and negative pressure differentials across the output piston; at the zero-crossing the switching of the hydraulic ports produces undesirable transient dynamics. A push–pull configuration is recommended, employing two such devices with one connected to each chamber of the output piston. This type of configuration is common in the analogous class-D amplifiers.

Finally, future work will seek to implement the above change while improving upon the fidelity of the component models. A full simulation will be performed, integrating the hydraulic device fully into the structural model. Experimental work will seek to verify the results of the simulation.

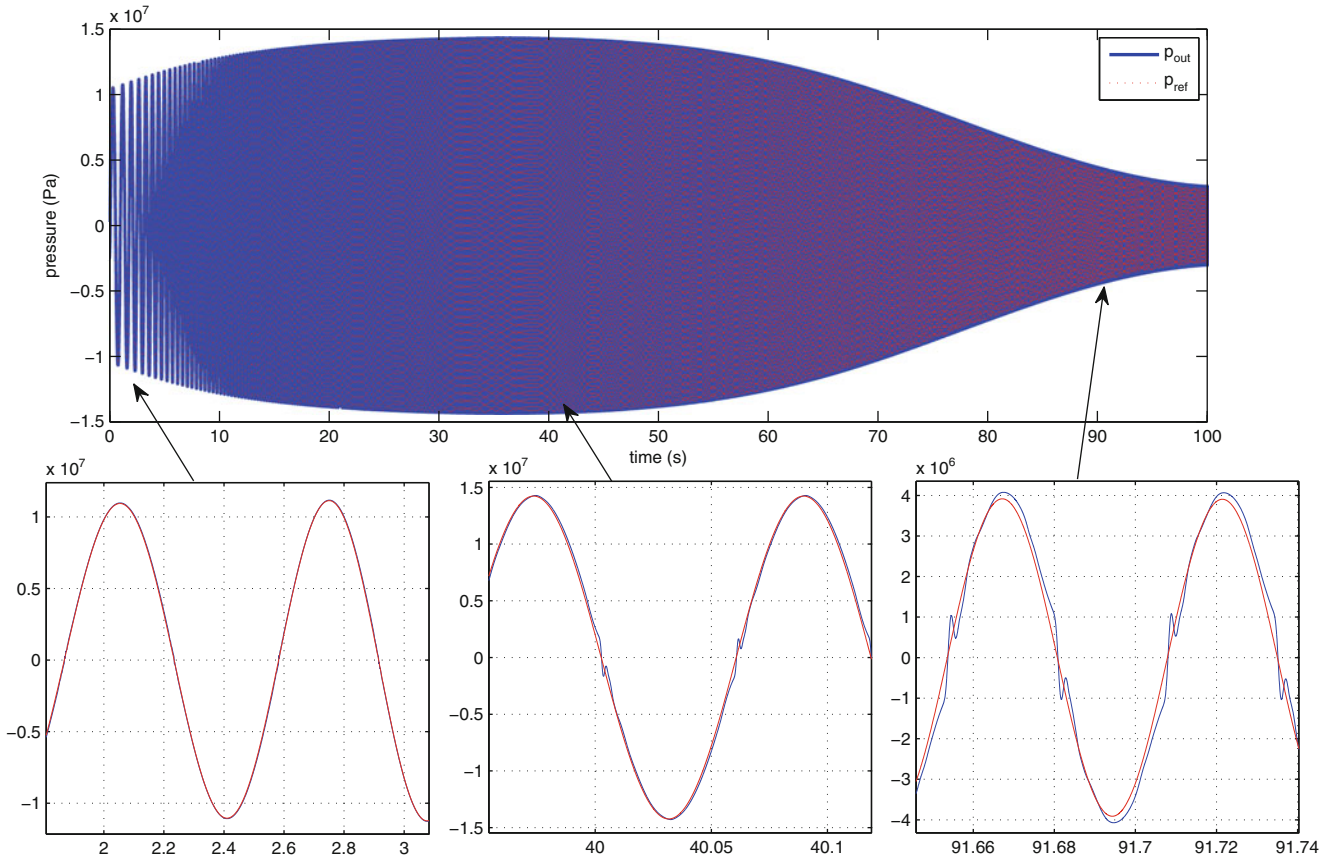


**Fig. 17.7** Reference and output pressure signals with tenfold increase in valve switching speed

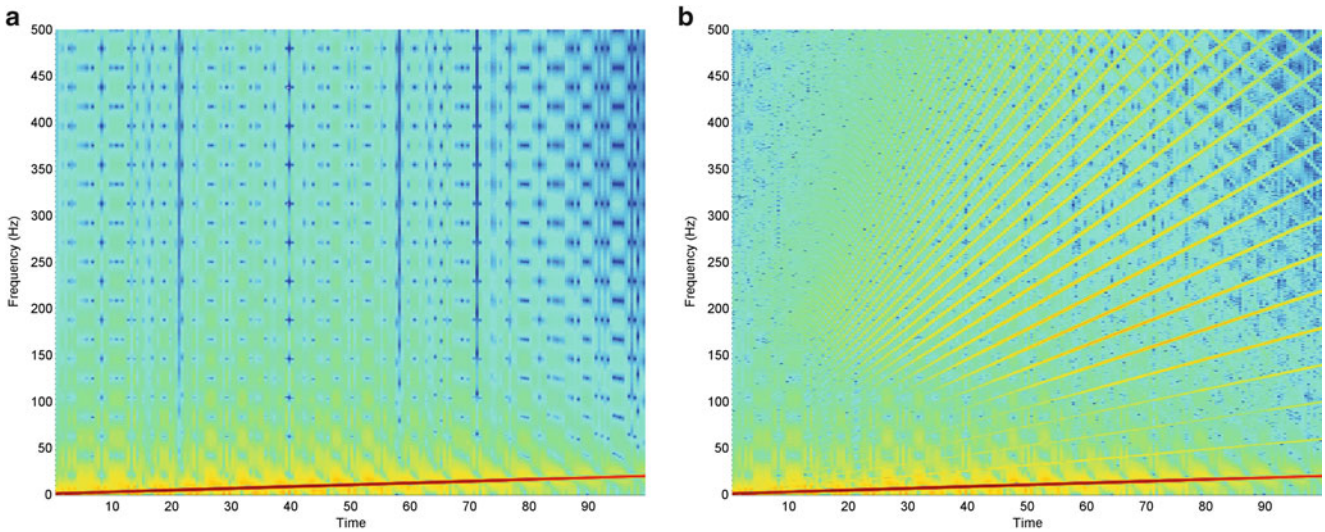


**Fig. 17.8** Spectral decomposition with a STFFT for the reference and output pressures of the hydraulic device with tenfold increase in valve switching speed. (**a**) Reference pressure; (**b**) output pressure

## References

1. Wagg D, Neild S (2010) Nonlinear vibration with control: for flexible and adaptive structures, vol 170. Springer, Berlin
2. Fuller CC, Elliott S, Nelson PA (1996) Active control of vibration. Access Online via Elsevier
3. Karnopp D (1995) Active and semi-active vibration isolation. J Mech Des 117:177

4. Okada Y, Harada H (1996) Regenerative control of active vibration damper and suspension systems. In: Proceedings of the 35th IEEE conference on decision and control, vol 4, pp 4715–4720
5. Suda Y, Nakadai S, Nakano K (1998) Hybrid suspension system with skyhook control and energy regeneration (development of self-powered active suspension). Veh Syst Dyn 29(S1):619–634
6. Nakano K (2004) Combined type self-powered active vibration control of truck cabins. Veh Syst Dyn 41(6):449–473
7. Pan M, Johnston N, Plummer A, Kudzma S, Hillis A (2013) Theoretical and experimental studies of a switched inertance hydraulic system. Proc Inst Mech Eng Part I J Syst Control Eng 228(1):12–25
8. Jeffery TD, Thomas TH, Smith AV, Glover PB, Fountain PD et al (1992) Hydraulic ram pumps: a guide to ram pump water supply systems. Intermediate Technology Publications, London, UK, ISBN 9781853391729
9. Lazar I, Wagg D, Neild S (2012) Reducing the clipping effect of semi-active clipped optimal control of a two storey building. In: ISMA2012 international conference on noise and vibration engineering, Leuven, Belgium, September 2012
10. Brogan WL (1991) Modern control theory, 3rd edn. Prentice-Hall, Englewood Cliffs
11. Sangiah DK, Plummer AR, Bowen CR, Guerrier P (2013) A novel piezohydraulic aerospace servovalve. Part 1: design and modelling. Proc Inst Mech Eng Part I J Syst Control Eng 227(4):371–389
12. Branson DT, Wang FC, Johnston DN, Tilley DG, Bowen CR, Keogh PS (2011) Piezoelectrically actuated hydraulic valve design for high bandwidth and flow performance. Proc Inst Mech Eng Part I J Syst Control Eng 225(3):345–359
13. Titurus B, du Bois J, Lieven N, Hansford R (2010) A method for the identification of hydraulic damper characteristics from steady velocity inputs. Mech Syst Signal Process 24(8):2868–2887